Fabrication of Randomly Integrated PMMA/ZnO nanorods NanoGenerator (RING)

Dr. Madunuri Chandra Sekhar[1]

Asst.Prof Physics,

Chaitanya Bharathi Institute of Technology

Hyderabad, Telangana, 507002

Eediga Nirmala Devi[2]

Research Scholar

Department of Physics

Rayalaseema University, Kurnool

Abstract:

An easy & efficient fabrication method of ZnO NanoGenerator, in which the Randomly oriented ZnO naorods are deposited on silver coated copper electrode was reported in this paper, besides, PMMA is spin coated over the randomly aligned ZnO nanorods for the intention of their enduring constancy. The ZnO nanorods tips from PMMA are covered by gold coated zigzag copper electrode. The performance is based on Metal-Semiconductor schottky barrier, the operation of RING (Randomly Integrated NanoGenerator) is analyzed by subjecting the two electrodes to minor relative displacements which produces an output of 0.9V. The random orientation of nanorods is revealed by the SEM images in PMMA. XRD, UV, FTIR, PSA, AFM further confirmed the presence and performance of ZnO nanorods in PMMA.

Keywords: ZnO nanorods, Piezoelectricity, PolyMethyl-MetaAcrylate, RING(Randomly Integrated NanoGenerator), Schottky barrier.
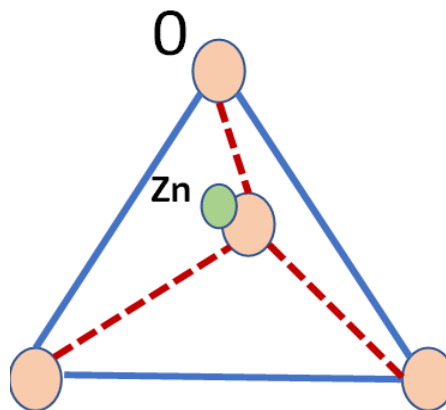

Fig 2a. Pzt effect in ZnO unit cell (P-dipole vector).

1. Introduction:

To produce energy from environment mechanical vibrations, nanopiezotronics are being developed and the same is stimulating a new overwhelm of research on self powered nanosystem[1-4]. A regular instance is the fabrication of ZnO nanogenerator which is relied on the piezoelectric effect [5]. The nanoscale mechanical energy is converted by the nanogenerator into electrical energy by using the coupling of PZT and semiconducting properties of ZnO nanorods. Integrated nanogenerator(LING),Vertically integrated nanogenerator(VING) are the most common nanogenerator structures.

An easy method was looked at by us to construct Randomly Integrated NanoGenerator (RING) that shows improved output voltage and current.

ZnO is a semiconducting piezoelectric material having energy band gap of 3.37eV and large excitation binding energy of 60meV at room temperature [6]. Exhibiting both semiconducting and piezoelectric properties those are eco friendly, biocompatible, easy growth methods are the benefits of ZnO nanostructures [7]. Various methods are used for the synthesis of ZnO nanostructures. Solution based chemical techniques are more beneficial as they are easy, handy, inexpensive, less dangerous, compatible for flexible/metal substrates, competent of large scaling up and development happens at relatively low temperature[6]. So in the current work, piezoelectric ZnO nanorod deposition on metal alloy substrate with flexible material like PMMA spin coated, has been reported, which brings robustness to the nanogenerators. M-S interface is the vital parameter for the working of nanogenerators.
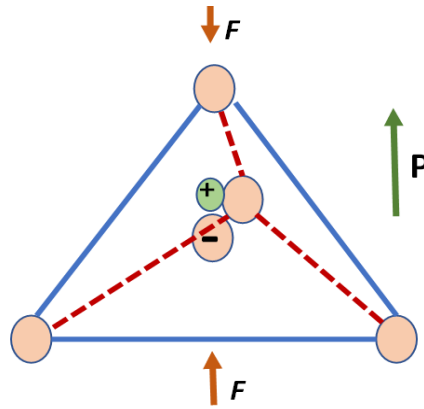
Fig 2b. Two operating modes for pzt material:
a) 33 mode b) 31 mode.

2. Piezoelectricity of ZnO

ZnO comes under the class of piezoelectric materials and its anisotropic piezoelectric properties are because of its crystal structure which belongs to $P6_3mc$ symmetry group having no center of symmetry [8]. In this case, the unit cell bary centers of positive and negative charges do not overlap. As shown in Fig 2a, the electric dipole will be appeared within the crystal and it modulated by the application of mechanical stress (direct piezoelectric effect).

The piezoelectric coefficient d_{ij} is the ratio of the strain in the j-axis to the electric field applied along the i-axis, when all external stresses are held constant. In the piezoelectric material there are two practical coupling modes: the stack configuration operating in the 33 mode and the bend configuration operating in the 31 mode as shown in Figure 2b. The sign convention assumes that the poling direction is always in the "3" direction.

d_{31} will be applied for the force applied in the direction perpendicular to the poling direction, such as bending,; and d_{33} will applied for the force applied in the identical direction as the poling direction, such as the compression. In 31 mode, the electric field is along the polarization axis (direction 3), but the strain is in the 1 axis (orthogonal to the polarization axis). In 33 mode, the electric field is along the polarization axis (direction 3). Typically, the 31 mode has been the regularly used coupling mode in the energy harvesting via piezoelectric effect, but the piezoelectric coefficient d_{31} is lower than d_{33}.

Based on its orientation the ZnO crystal is anisotropic; its piezoelectric coefficients are dissimilar. d_{33} =12.4 pm/V is the accepted piezoelectric coefficient of single crystal ZnO [9], d_{31}= 5.1 pm/V is also reported [10]. Due to the high aspect ratio ZnO nanowires/nanorods can endure larger amounts of strain to generate more mechanical energy accessible for conversion into electrical energy.
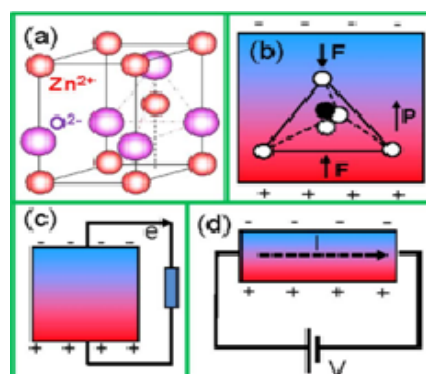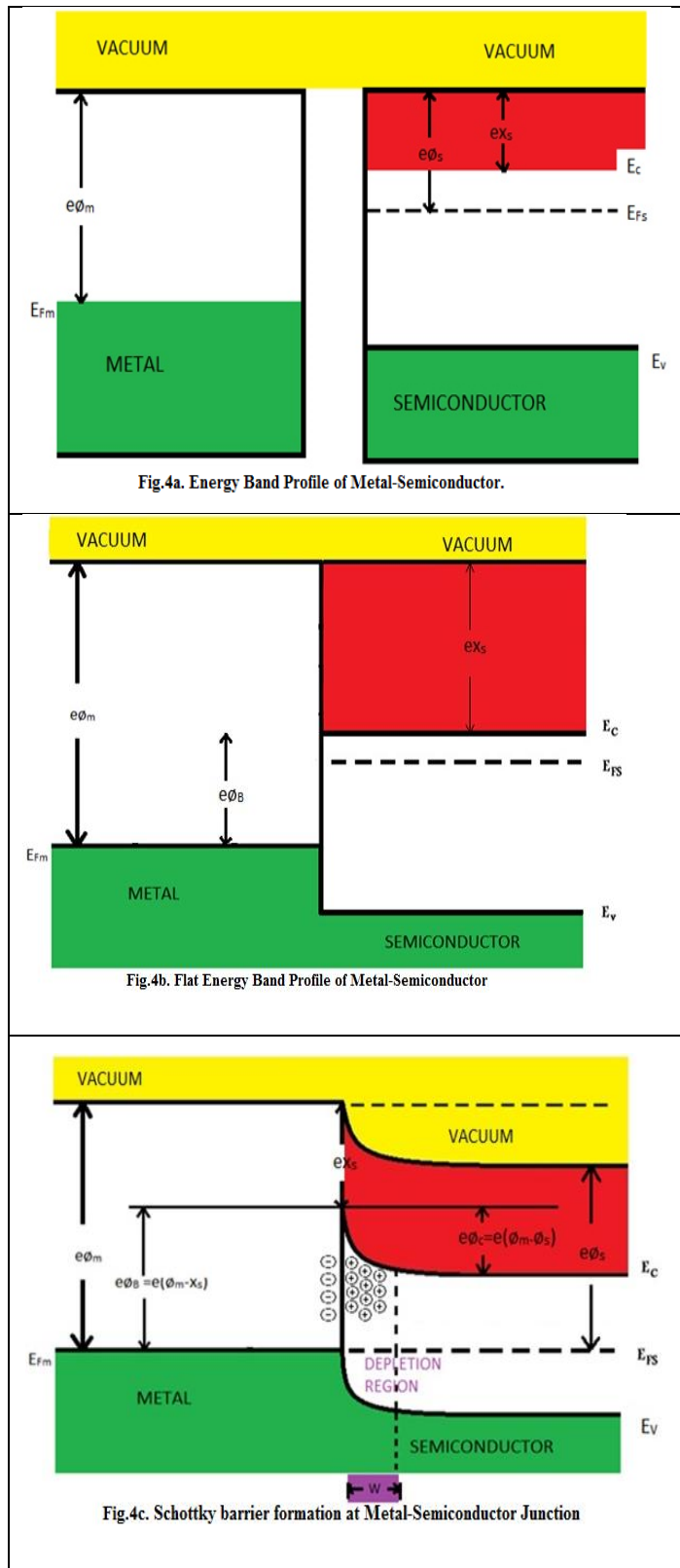
3. Primitive Regulation of Nanogenerator

Fig 3 (a) wurtzite structured ZnO.
(b) Piezopotential of a Stretched ZnO NW.
(c) Power generation with the piezopotential.
(d) Current variation in a semiconductor by piezopotential.

As shown in Figure 3(a), ZnO has the wurtzite structure, where the tetrahedral coordinated O^{2-} and Zn^{2+} are stacked layer by layer along the c-axis. The ZnO structure is deformed so that the charge centers of Zn^{2+} cations and O^{2-} anions separate and result in an electric dipole shown in Figure 3(b), when an external strain is applied the piezoelectric field is preserved as long as the NW/NR

is strained[11,12]. The electrons in the circuit are driven to flow to partially screen the piezopotential after a strained crystal is connected to an external load which is the method for converting energy. Therefore the norm of the nanogenerator is the transient flow of electrons in outer load as driven by the piezopotential created by dynamic straining shown in Figure 3(c) whereas, the piezopotential acts as a gate voltage that can tune/gate the transport process of the charge carriers under the driving force of an externally applied voltage shown in Figure 3(d) if the material is also a semiconductor. According to the principle of metal and semiconductor junction (Schottky junction) the device fabricated can be known as the piezotronic device[13].

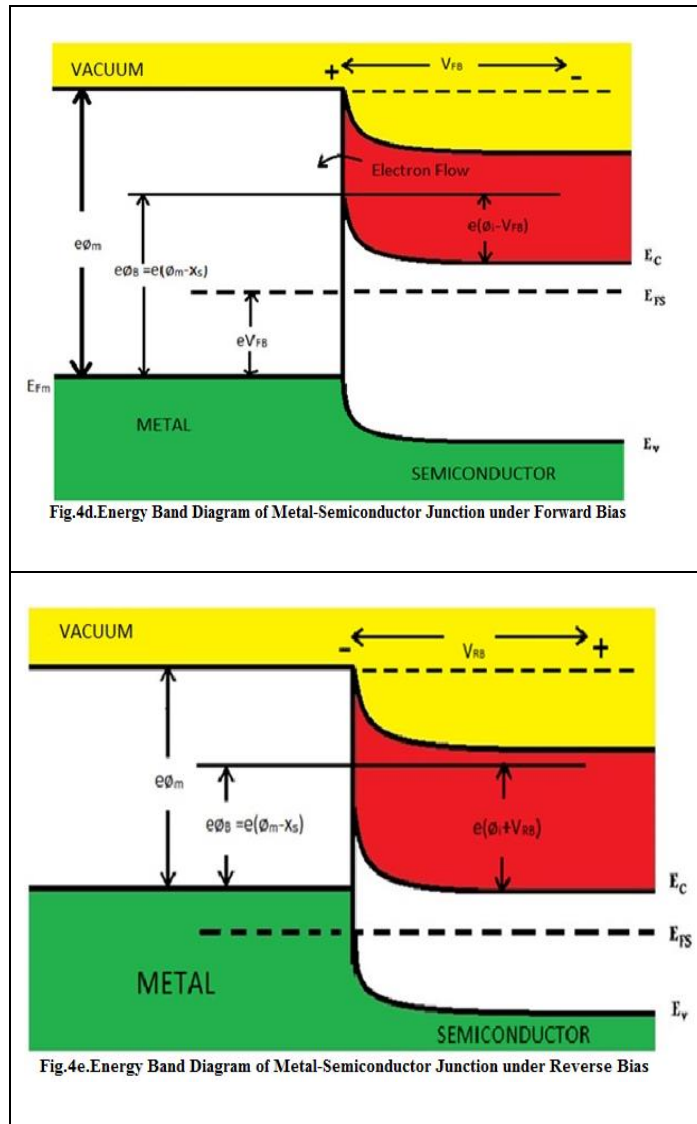## 4. Schottky Junction or Metal-Semiconductor Junction :

Fig.4a. Energy Band Profile of Metal-Semiconductor.

Fig.4b. Flat Energy Band Profile of Metal-Semiconductor

Fig.4c. Schottky barrier formation at Metal-Semiconductor Junction

Fig.4d.Energy Band Diagram of Metal-Semiconductor Junction under Forward Bias

Fig.4e.Energy Band Diagram of Metal-Semiconductor Junction under Reverse Bias

Metal - semiconductors junctions are the necessary characteristic of nanoelectronic devices. As shown in the Figure 4(a) the work function (ϕ_m) is the energy needed to take away electron from the Fermi level of the metal to vacuum level, the energy needed to remove an electron from the conduction band to the vacuum level of semiconductor is known as electron affinity χ_s .

In metals the Fermi energies of the metal do not vary at once as the metal and semiconductor are brought collectively [13]. As shown in the Figure 4(b) this yields the flat band diagram. A barrier of electrons will be formed by a metal-semiconductor junction, if the Fermi energy of the metal is somewhere between the conduction and valance band. A dispersion of the electrons will happen from the semiconductor to the metal. A decreased electron concentration in the semiconductor is left by the net transfer of the electrons and procedure goes on until E_{FS} constant. As electrons are reduced from the semiconductor a creation of net positive charge is visible in the semiconductor at the junction.

Schottky barrier which is a potential barrier of $e\phi_B = e\phi_m - e\chi_s$ is formed at the M-S interface. As shown in Figure 4(c), when these two forces are equivalent then equilibrium is set up. In response to the forces just explained, notice that the semiconductor energy bands bend [14]. The amount of band bending can be called the built in potential $e\phi_i$. At equilibrium for an electron to cross from the semiconductor to metal it over comes $e\phi_i$.

The barrier potential $e\phi_B$ must be overcome, to cross from the metal, for an electron to semiconductor. Consider a positive external potential (FB) is applied such that this will create an electric field across the junction then the diffusion current will not be opposed and current flows across the junction. Note the reduction in barriers for electron flowing from semiconductor but not for electron flowing from metal to semiconductor as shown in figure 4(d). With respect to the Fermi energy semiconductor the E_{FM} of metal is lower [14].

The metal's Fermi energy is increased with respect to the Fermi energy in semiconductor if a negative voltage (RB) is applied to the metal as shown in Figure 4(e). At the junction the electric field is reinforced by the external field caused by the reduced carriers increased the band bending and stop the diffusion current from flowing [15]. With positive barrier height the metal-semiconductor junction acts as rectifying behavior. In this way a semiconductor to metal barrier is decreased in forward bias and increased in reverse bias.

Table. 8.2 . Work function, electronic affinity of metals.

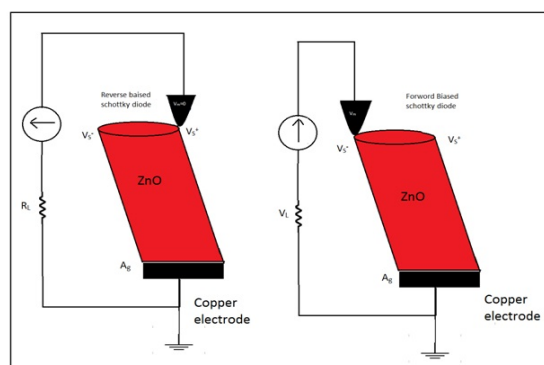| Some metals Work function	
Element	**Work function ϕ_m volts**
Ag , silver	4.26
Au , Gold	5.1
Pt , Platinum	5.65
Pd, Palladium	5.12
Ni , Nickel	5.15

Fig.5.Power generation process of a piezoelectric ZnO nanorod as a result of coupled piezoelectric and semiconducting properties with the Schottky barrier at copper tip-ZnO nanorod interface.

Some metals Electron affinity	
Element	**Electron affinity χ_s volts**
Ge , Germanium	4.13
Si , Silicon	4.01
GaAs , Gallium Arsenide	4.07
AlAs, Aliminium Arsenide	3.5
ZnO , Zinc Oxide nanorods	4.5

5. Nanogenerator's Working Module

The contact at top and bottom ends should be asymmetric: one Ohmic and one Schottky, to gain the harvesting energy output [16]. The electron affinity (χ_s) of ZnO is 4.5 eV and the work function (ϕ_m) of polycrystalline paste Ag is 4.2eV ($\phi_m < \chi_s$), hence there is no barriers at the interface Ag/ZnO leading an Ohmic contact[17]. The top end contact Au coated Cu/ZnO in which Au has a ϕ_m of 5.4eV ($\phi_m > \chi_s$), the entire transport procedure is dominated by a Schottky barrier which was shown in such system on the other side [18].

There are two diverse transport procedures across the Au coated Cu/ZnO Schottky barrier because of the two contrary potentials from the compressed side (negative potential V_s^-) and the stretched side (positive potential V_s^+) of the ZnO NR. The tip will first enter in contact with the stretched surface where $V_s > 0$, so the Au coated Cu metal tip has a potential $V_m \approx 0$ leading a negative bias at the metal tip Au coated Cu/semiconductor ZnO interface $\Delta V = V_m - V_s^+ < 0$, at the time of Au coated Cu tip scan. Therefore as shown in Figure.5 (a) the interface is a reverse biased Schottky diode and in such case, only small current flow can be across the interface because of the n-type semiconductor features of the ZnO NRs. Second, interface is a forward biased Schottky barrier, when the Au coated Cu tip enters in contact with the compressed side of the NW where $V_s < 0$, leading a positive bias at the same interface $\Delta V = V_m - V_s^- > 0$, the ZnO NR based NG can save the piezoelectric charges and later produce the discharge output.

6. Experimentation for Nanogenerator

Copper is, generally, a thin and economical fine electrical conductor for the fabrication of **Randomly Integrated NanoGenerator (RING)**. From the copper plate, so as to stop the ZnO nanorod's detachment, at the boundary interface under an applied strain, Cu plate's micro scale coarse surface was rubbed with sandpaper, cleaned chemically and immersed in electrolyte for electro deposition of ZnO nanorods on to it. There is a uniform or random deposit of ZnO Nanoparticles and nanorods together with lateral, vertical, tilted nanorods on the copper substrate in large area, later it is spin coated with a few micrometers layer of PMMA on ZnO nanostructures as one type of sample and another plate coated with PMMA/ZnO nanocomposite prepared previously. Afterwards 90 seconds of oxygen plasma etching is performed to etch out the PMMA coating's fine thickness for the reason of top electrode contact and the nanorods tips are projected out to some extent. Thus the PMMA coated on ZnO nanostructures are further covered by another zigzag copper plates on each which acts as another electrode. We named it **Randomly Integrated NanoGenerator (RING)** as the copper plate was randomly deposited by nanorods. The voltage from a single nanowire was not measured by the measurement of output voltage of a ZnO nanogenerator , instead from the nanogenerator as a whole .

7. Results And Discussions

7.1. XRD Analysis

Figure 7.1. XRD spectra of PMMA coated on ZnO structures.
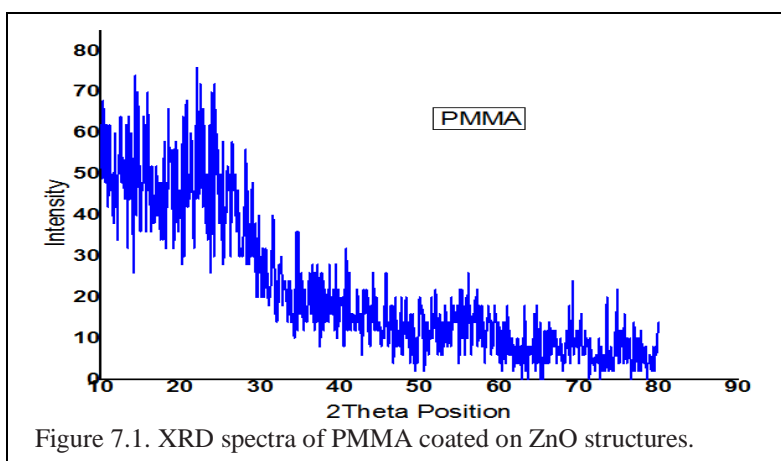
We recorded PMMA's X-ray diffraction patterns on ZnO Nanostructures. As shown in Figure 8.26, a broad non crystalline peak $(10–30^0)$ of PMMA and nanocrystalline diffraction peaks $(30–80^0)$ of ZnO were shown by the XRD patterns. The ZnO nanostructure's incorporation generates neither a new peak nor a peak shift by means of PMMA indicating two phase structures.

7.2 FTIR Analysis

The FTIR spectra of the films are equivalent except for the absorption peaks at 3410 cm^{-1}, which are assigned to Acrylate carboxyl group on the ZnO surface. The films display the feature, strong absorption peaks of 1742 and 1150 cm^{-1}, which are caused by CAOAC stretching of the PMMA linkages. The absorption peak at near 1447 cm^{-1} is attributable to represent the bending, stretching of CH$_2$ and CH$_3$ group in PMMA. The ZnO nanostructures' incorporation in PMMA matrix is confirmed by appearance of characteristic Zn-O vibration band at 459cm^{-1}.

Fig 7.2. FTIR spectra of PMMA coated on ZnO structures.
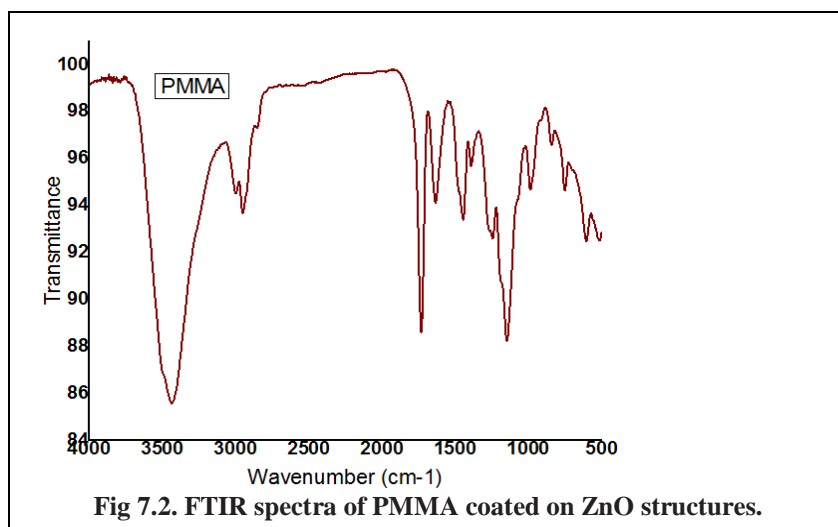
7.3 UV Analysis

Figure 7.3 shows the UV-V which is the spectra of PMMA coated on ZnO nanostructures in the spectral range between 220nm and 385nm.The absorption peak is seen at 372nm corresponding to the exciton state in the ZnO nanostructures. Visible transparency had been enhanced by PMMA coated on ZnO nanostructures films those are formed by the polymerization while UV absorption is still close to 100% of the incident UV light.
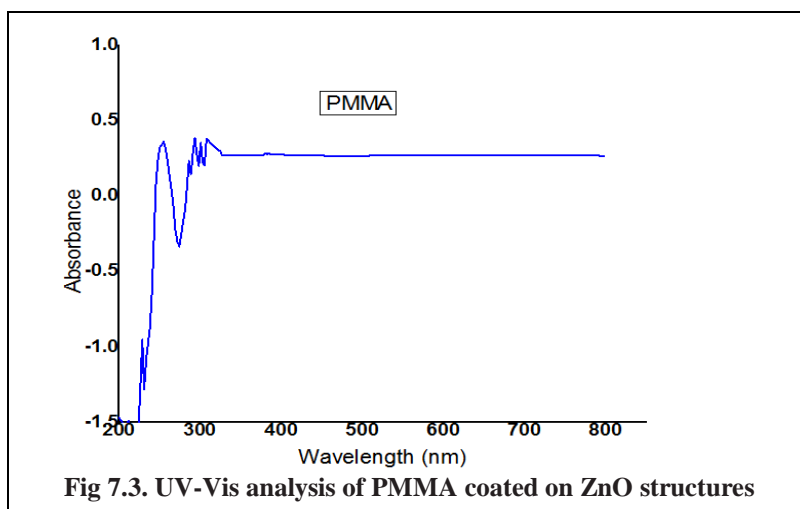

Fig 7.3. UV-Vis analysis of PMMA coated on ZnO structures

7.4   PSA Analysis

Figure 7.4 shows the results of size distribution measurements of PMMA coated on ZnO nanostructures. It could be inferred that nanostructures' cumulated diameters in effect is intense micro mixing by sonication. The nanostructures' average size in PMMA are within the range of 56 nm, a slight difference from the size of individual nanostructures i,e 42nm. Aggregation of ZnO structures is the probable cause for particle size distribution's
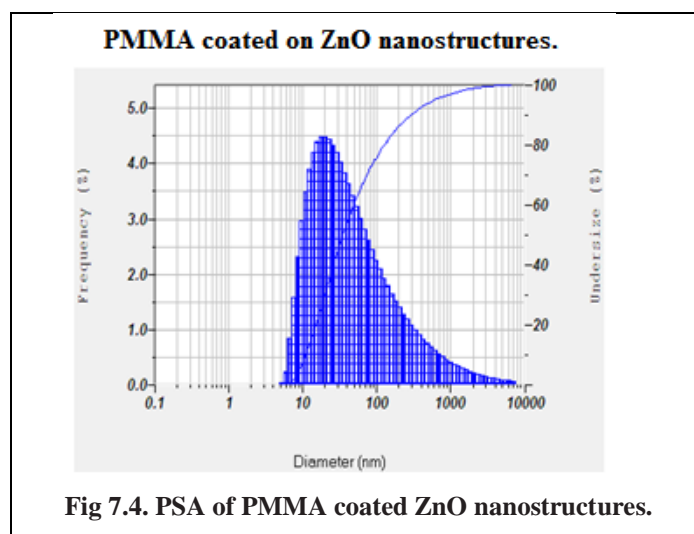
increase.

Fig 7.4. PSA of PMMA coated ZnO nanostructures.

7.5.RAMAN Analysis :

Raman Spectrometer is used to study Raman spectra over the range 0 - 4000 cm^{-1}. Here it is monitored that the maximum intensity takes place at around 1060.33 cm^{-1} for the PMMA coated on ZnO nanostructures. The outcomes disclosed that the weaker Raman peaks in between 1000cm^{-1} to 1500cm^{-1} are because of the interactions of zone-boundary phonons arising owing to both C-H and Zn-O nanostructures 'stretching vibrations f in the composite.
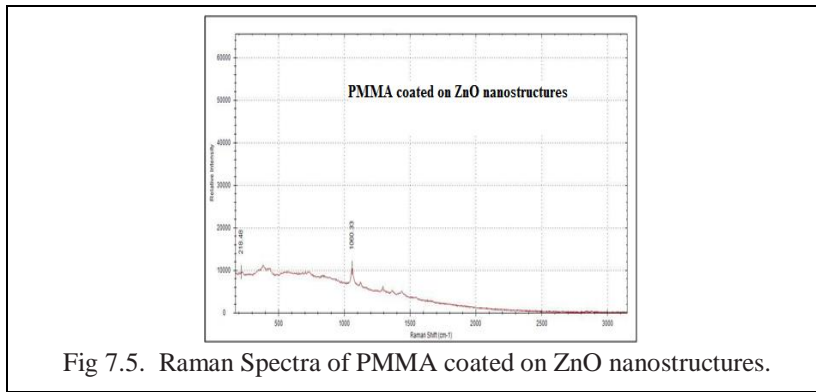
Fig 7.5. Raman Spectra of PMMA coated on ZnO nanostructures.
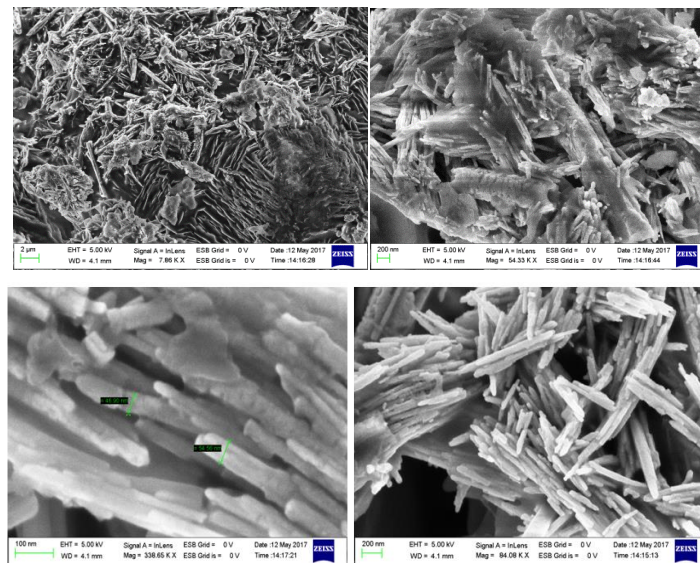
7.6 SEM Analysis

Fig 7.6. SEM images of PMMA coated on ZnO Nanostructures.

Figure 7.6 shows PMMA's SEM images on ZnO nanostructures. PMMA's spin coating is done for the reason of long term nanorods' stability and complete nanogenerator structure's mechanical robustness. Also, it assists to put off possible short circuiting between the bottom and the top electrodes. Later, 90 seconds of oxygen plasma etching is done to etch out the fine PMMA's coating thickness for the purpose of top electrode contact and the nanorods tips are somewhat projected out as shown in Figure 7.6. From the figure it is disclosed that the Nanorods are randomly deposited and the PMMA layer between the nanorods serves as an insulator. The nanorods tips which are somewhat projected out are the key factor for the production of current when brought in contact with the zigzag electrode that was gold coated.
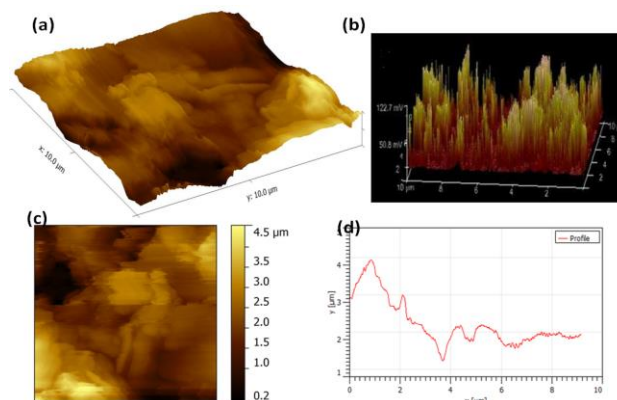
7.7. Atomic Force Microscope Analysis

Fig.7.7.2. AFM image of PMMA coated on ZnO Nanorods deposited sample.

The PMMA's topography coated on ZnO nanorods deposition sample which discloses that the surface is having high roughness as compared to earlier sample is shown in Figure 7.7.2(a). The PMMA's three dimensional current image coated on ZnO substrate which shows piezoelectric potentials of ZnO which is low compared to composite i.e. in 120-150mV because of proper dispersion of PMMA on ZnO nanorods or plasma etching is shown in Figure 7.7.2(b). The topography image of the low bending distance and the mechanism behind the generation of piezoelectric potential which is due to direct coating of PMMA hindering the bending moment of ZnO nanorods.

8. CONCLUSION:

The piezoelectric and semiconducting properties' combination, i.e. piezotronic effect of ZnO nanostructures, set the foundation for a new procedure: piezotronics. The random integration of NRs gives a realistic procedure way for NG nanoinstruments towards original applications to convert mechanical energies to electricity effectively. On copper plates the ZnO nanorods' orientation was revealed by UV, XRD, RAMAN, FTIR, SEM,AFM analysis. By connecting digital oscilloscope, the performance of NG can be studied.

REFERENCES:

[1] Z.L.Wang, Nano Today 5, 512 (2010).

[2] C.Chang, V.H.Tran, J.B.Wang, Y.K.Fuh and L.W.Lin, Nano Lett. 10,726 (2010).

[3] S.N.Cha, J.S.Seo, S.M.Kim, H.J.Kim, Y.J.Park, S.W.Kim and J.M.Kim, Adv.Mater. 22,4726 (2010).

[4] X.Y.Wang, K.Kim, Y.M.Wang, M.Stadermann, A.Noy, A.V.Hamaza, J.H.Yang and D.J.Sirbuly, Nano Lett. 10,4901 (2010).

[5] Z.L.Wang and J.H.Song, Science 312, 246 (2006).

[6] Sh.Xu, Z.L.Wang, Nanao Res.Review Article (2011).

[7] Sh.Xu, Y.Qin, Chen Xu, Y.Wei, Rusen Y, Z.L.Wang, Nature Nanotechnology, Vol 5, PP 366-373, (2010).

[8] Kong X.Y., Wang Z.L., "spontaneous polarization induced helixes, nanosprings and nanorings of piezoelectric nanobelts", nano letters,vol.3,pp.1625-1631,2003.

[9] Christman J.A., Woolcott R.R., Kingon A.I.et al., "Piezoelectric measurements with atomic microscopy", Journal of Applied Physics Letters, vol 73, p.3851,1998.

[10] Bernardini F., Fiorentini V.,Vanderbilt D.," Spontaneous polarization and piezoelectric constants of III-V nitrides". Physical Review B, vol.56, p.R10024,1997.

[11] J. Zhou, P. Fei, Y.D. Gu, W.J. Mai, Y.F. Gao, R.S. Yang, G. Bao, Z.L. Wang, Nano Lett. 8(2008) 3973.

[12] J. Zhou, Y.D. Gu, P. Fei, W.J. Mai, Y.F. Gao, R.S. Yang, G. Bao, Z.L. Wang, Nano Lett. 8(2008) 3035.

[13] K.A.Christianson, "Contribution of surface and Interface states to the reverse biasing of Schottky barriers," 1990 GaAs REL Workshop Digest. Oct.7,1990.

[14] S.M., Physics of semiconductor Devices, John Wiley & Sons,Newyork,1981.

[15] Yang E.S., Fundamentals of Semiconductor Devices, Mc Graw Hill Book company, Newyork,1978.

[16] Wang Z.L., Kong X.Y., Zuo J.M., "Induced growth of asymmetric Nanocantilever arrays on polar surfaces", Physical Review Letters, vol.91,p.185502,2003.

[17] Wang Z.L., "Piezoelectric nanostructures: from novel growth phenomena to Electric nanogenerators", MRS Bulletin, vol. 32, pp.109-116, 2007.

[18] Wang X., Song J., Liu J. et al., "Direct current nanogenerator driven by ultrasonic waves" Science, vol. 316, pp. 102-105,2007.

[19] Wang Z.L., Nanogenerators for self powered devices and systems, SMARTech digital repository, Georgia Institute of Technology, Atlanta, GA, 2011.